

Matrix remodeling associated 5 expression in trunk and limb during avian development

J. ELI ROBINS and ANTHONY A. CAPEHART*

Department of Biology, East Carolina University, Greenville, NC, USA

ABSTRACT Matrix remodeling associated 5 (MXRA5) is an extracellular protein that is upregulated in several cancers, but little is known regarding its spatial and temporal localization in the developing embryo. The present study was undertaken to investigate MXRA5 transcript expression in the trunk and limb of the embryonic chick to provide groundwork for future investigation of its developmental function. *In situ* hybridization utilizing digoxigenin-labeled sense control and experimental antisense probes was performed in paraffin sections of chick embryos from Hamburger and Hamilton (HH) stages 18-38. MXRA5 expression was initially low and restricted in extent at the earliest stages examined, but expression increased in strength and tissue distribution with developmental age. Transcripts were largely found in cells of mesodermal origin, including gut associated mesenchyme, tendon and ligament rudiments, intervertebral discs, dermal papillae of feather buds, heart valve precursors and leaflets, as well as in appendicular joint primordia. The present study has provided initial information on MXRA5 gene expression in the trunk and limb of early to mid-stage avian embryos. Results show that MXRA5 was expressed most strongly at sites undergoing change and remodeling of the extracellular matrix during transition of embryonic tissues into the functional adult morphology.

KEY WORDS: *MXRA5, chick embryo, heart development, limb development*

Matrix remodeling associated 5 (MXRA5), originally termed adican, was assigned to the MXRA family based on co-expression with known adhesion and remodeling genes (Walker and Volkmuth, 2002). MXRA5 is proposed to be a secreted protein involved in protein:protein interactions containing seven leucine-rich repeats (LRR) along with twelve immunoglobulin-like domains and also subsequently assigned to the extracellular LRR superfamily (Dolan *et al.*, 2007). Although its precise function has not yet been clearly defined there is strong correlation of increased MXRA5 expression with colon, ovarian, lung, and other cancers (Zou *et al.*, 2002; Buckanovich *et al.*, 2007; He *et al.*, 2015). In addition to involvement in tumor growth, MXRA5 protein has also been found associated with pathologies such as osteoarthritis where it was found to be secreted into synovial fluid (Balakrishnan *et al.*, 2014).

Our lab's interest in MXRA5 is based on results of microarray experiments in which versican chondroitin sulfate proteoglycan expression was knocked down in developing synovial joint primordia of HH25-35 (Hamburger and Hamilton, 1951) chick wings (Nagchowdhuri *et al.*, 2012) which resulted in significant (2.2-fold) reduction of MXRA5 transcripts. It was thus necessary to verify expression of MXRA5 in relevant tissues during joint morphogenesis

prior to investigation of its function and potential interaction with versican. It has been reported previously that MXRA5 is expressed by a chick embryonic fibroblast cell line (Kong *et al.*, 2011) and in late stage chick intestinal tissue (Soulett *et al.*, 2013), as well as in mesenchymal stem cells derived from human umbilical cord blood (Joyce *et al.*, 2012), however, there is currently a paucity of information regarding cellular localization of MXRA5 with regard to the developing limb or elsewhere in early stages of the embryo. Since little is known regarding temporal and spatial expression of MXRA5 during embryonic development we initiated the present study to investigate its expression in trunk and limb of the developing chick. Understanding the spatial and temporal localization of MXRA5 during embryogenesis will provide a basis for experiments to explore its developmental function and perhaps offer insight into

Abbreviations used in this paper: AV, atrioventricular; ECM, extracellular matrix; HH, Hamburger and Hamilton stage; LTBP2, latent transforming growth factor beta binding protein 2; LRR, leucine-rich repeats; MXRA5, matrix remodeling associated 5; OT, outflow tract; RT-PCR, reverse transcriptase-polymerase chain reaction; SSC, saline sodium citrate; TBS, tris buffered saline; TGF β , transforming growth factor beta.

*Address correspondence to: Anthony A. Capehart. Department of Biology, N108 Howell Science Complex, East Carolina University, Greenville NC 27858, USA. Tel: +1-252-328-6296. Fax: +1-252-328-4178. E-mail: capehartt@ecu.edu

Submitted: 1 September, 2017; Accepted: 6 November, 2017.

its activity in mesenchymal stem cell populations and role in the growth and progression of various tumors.

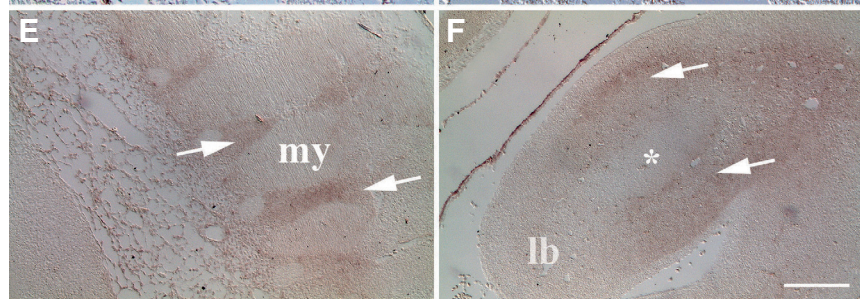
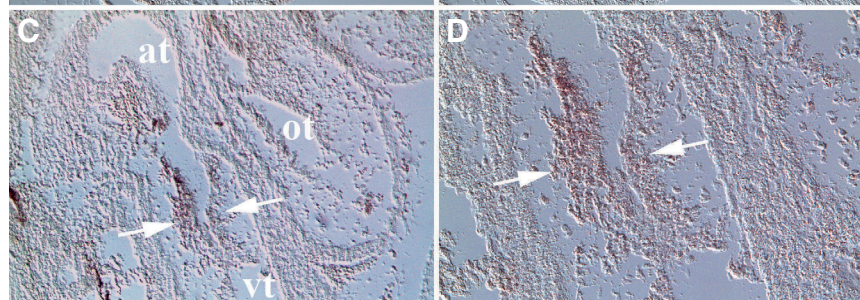
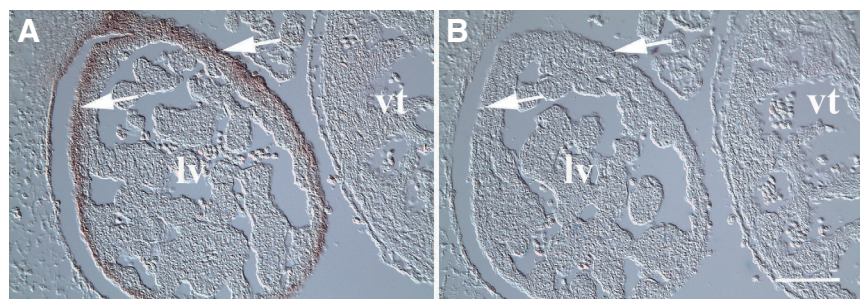
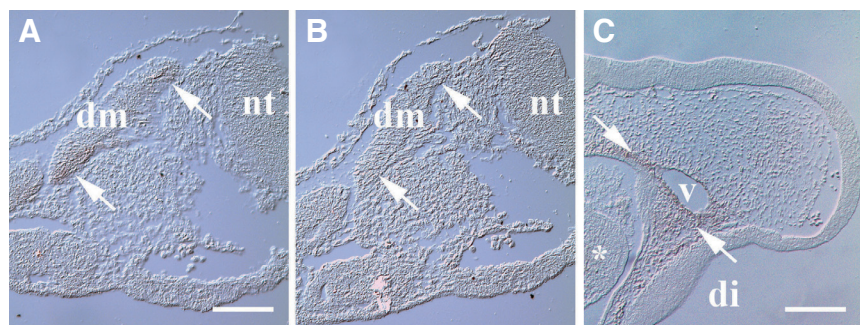
Results

HH18

MXRA5 transcripts were first detected weakly at HH18 and were limited largely in the trunk to dorsomedial and ventrolateral dermamyotome edges (Fig. 1A). Mesenchymal expression immediately surrounding vasculature was also seen associated with cranial vessels anterior to the trunk (Fig. 1C). Little MXRA5 expression was noted elsewhere at HH18 other than low level MXRA5 mRNA in cells along the periphery of the developing liver rudiment (not shown). Control specimens exposed to sense control probes lacked reactivity at HH18 (Fig. 1B) and later stages examined (Figs. 2B, 3B, 5I).

HH24/25

By HH24/25 widespread MXRA5 expression in liver-associated ventral mesentery was quite clear (Fig. 2A,B). One of the most striking sites of expression was in the heart (Fig. 2C,D), where strong staining was observed in atrioventricular (AV) mesenchyme populating the endocardial cushions. Little evidence of MXRA5 mRNA was seen during earlier stages of epithelial - mesenchymal transformation in AV cushions prior to this abrupt onset of overt expression at HH24/25. In the outflow tract (OT), weak staining of cushion mesenchyme was noted at this developmental stage. Pronounced MXRA5 expression elsewhere in the trunk included sites of segmental somitic musculature attachment (Fig. 2E) and scattered staining of adjacent loose mesenchyme in the abdominal wall. In leg buds MXRA5 transcripts were absent in the chondrogenic core, but prevalent in surrounding mesenchyme of the proximal limb (Fig. 2F).



HH28

At HH28, the most obvious changes in MXRA5 expression occurred in heart and limb that correlated with the significant morphological events taking place within those structures at this stage (Fig. 3). Strong MXRA5 localization in AV mesenchyme followed fusion of cushions and incipient remodeling into valvular tissues (Fig. 3A-C). Interestingly, MXRA5 staining was not uniform across AV cushions, but more intense toward the atrial aspect. In the OT, MXRA5 levels were again lower than observed in AV cushions and marked by patchy localization in discrete regions of proximal and distal OT cushion tissue (Fig. 3A,D). In the wing bud, MXRA5 transcripts were localized in perichondrial tissue surrounding the cartilaginous humeral anlage. Varying levels of expression were

Fig. 1 (top row). Limited MXRA5 mRNA expression in the HH18 embryo. (A) Transcripts were noted in primaxial and abaxial dermamyotome (dm) lips of trunk somites (arrows). nt, neural tube. (B) Sense control probe was unreactive in dermamyotome. (C) Low level expression was also observed in head mesenchyme surrounding vessels (v). Asterisk, first pharyngeal arch. di, diencephalon. Scale bar in (A), 100 μ m for (A,B); bar in (C), 200 μ m.

Fig. 2 (left). MXRA5 transcripts were noted at several sites in trunk and limb of the HH24/25 embryo. (A) Arrows show MXRA5 expression in mesentery covering the liver (lv). vt, ventricle. (B) Control probe did not exhibit reactivity with developing liver. (C) Expression in atrioventricular cushion tissue of the heart (arrows). At, atrium; ot, outflow tract. (D) Higher magnification of atrioventricular cushion tissues shown in B. Note specific reactivity within cushion mesenchyme. (E) Expression (arrows) was also localized at sites of myotome (my)-derived segmental musculature attachment. Reactivity was also observed in scattered cells in underlying loose mesenchyme of the posterior abdominal wall. (F) Expression in leg bud (lb) mesenchyme (arrows) surrounding the chondrogenic limb core (asterisk). Surrounding amnion was also reactive for MXRA5. Scale bar in (B), 100 μ m for (A,B,D); bar in (F), 200 μ m for (C,E,F).

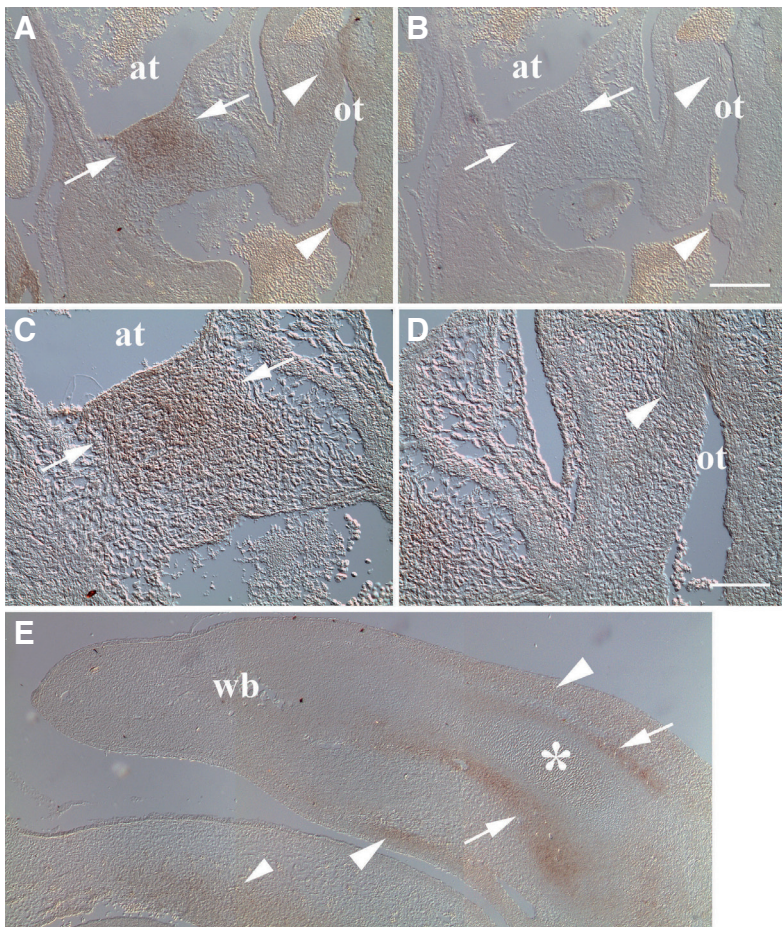


Fig. 3. MXRA5 mRNA expression in developing heart and limb at HH28. (A) Mesenchyme of fused atrioventricular cushions showed expression (arrows) particularly toward the atrial (at) aspect. Outflow tract (ot) cushion mesenchyme exhibited weaker and differential expression along its length (arrowheads). (B) Control specimens showed little or no reactivity in endocardial cushion tissues. (C & D) Higher magnification of atrioventricular and outflow tract cushion MXRA5 expression, respectively, shown in A. (E) Transcripts were localized in perichondrium (arrows) of the wing bud (wb). Note lack of signal in cartilaginous limb core (asterisk). Weaker reactivity was also noted in the developing dermis (larger arrowheads) as well as in adjacent body wall mesoderm (smaller arrowhead). Scale bar in B = 200 μ m for A, B, E; D = 100 μ m for C, D.

also noted in the presumptive dermis of the proximal limb flanking developing skeletal muscle masses (Fig. 3E) perhaps foretelling formation of dermal condensations during feather bud induction in ensuing stages (Yu *et al.*, 2004). At HH28, MXRA5 expression also continued in the trunk with a general trend toward more widespread localization at several sites such as body wall mesenchyme (e.g., bottom of Fig. 3E).

HH35

At HH35 MXRA5 mRNA exhibited robust localization in forming valve tissue of the AV septum and along the lateral aspect of AV canals (Fig. 4 A,B). The most intense signal was noted in cells immediately adjacent to the AV canals and biased somewhat toward the atrial side. Elsewhere in the HH35 trunk low level MXRA5 expression was also observed in the developing adventitia of the esophagus (Fig. 4C). As seen at earlier stages, small clusters of mesenchyme at various sites in the trunk also exhibited weak MXRA5 positivity, including cells within the forming pleural lining of the lung (Fig. 4C). Interestingly, MXRA5 expression within the liver mesentery, which was among the first sites where MXRA5 transcripts were localized,

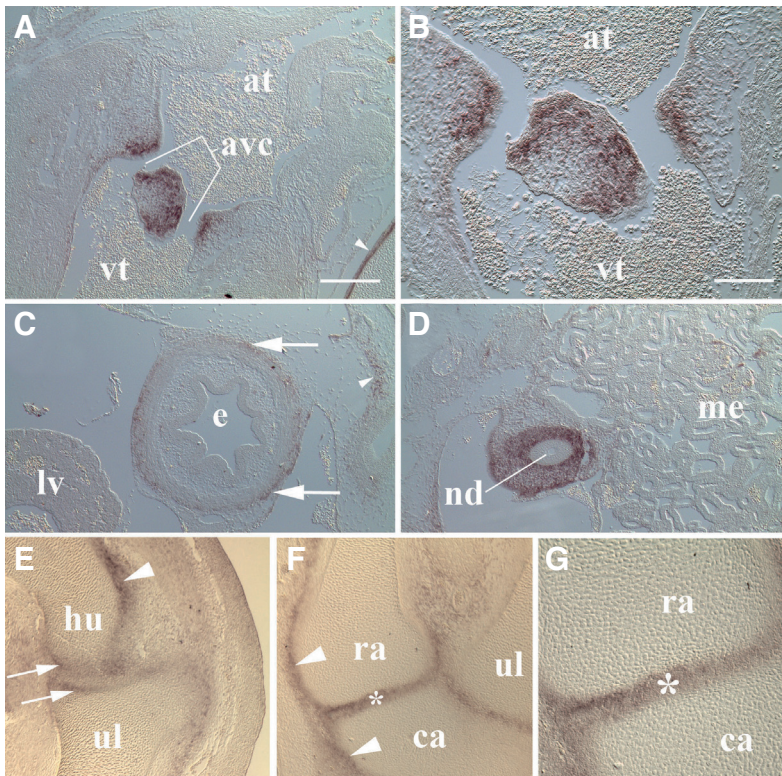


Fig. 4. MXRA5 mRNA expression in trunk and limb at HH35.

(A) Forming valve tissues lining the atrioventricular canals (avc, bracket) showed strong staining for MXRA5 transcripts. Note also sternal perichondrial staining (arrowhead). at, atrium. vt, ventricle. (B) Higher magnification of atrioventricular region shown in A. MXRA5 mRNA was largely found in cells lining the atrioventricular canals. (C) Low level staining was seen in adventitia (arrows) covering the esophagus (e). Note liver (lv) mesentery no longer displayed MXRA5 localization at this stage. Weak signal was also noted in small clusters of nearby mesenchyme associated with pleural covering of the lung (arrowhead). (D) Reactivity was pronounced in mesoderm surrounding the nephric duct (nd). me, mesonephros. (E) Transcripts in cells of the presumptive humeral (hu) and ulnar (ul) articular surfaces of the developing elbow joint (arrows). Differential perichondrial staining was also seen along surfaces of humeral (arrowhead) and ulnar cartilages. (F) Robust localization in pre-cavitation interzones of the wrist (asterisk). Asymmetric perichondrial staining was again noted along distal radial cartilage and continued along carpal cartilage (arrowheads). ra, radius. ca, carpal. (G) Higher magnification of radiocarpal articular anlage in F with MXRA5 localization in interzone cells. Scale bar in (A), 200 μ m for (A,C,D,E,F); bar in (B), 100 μ m for (B,G).

was absent at HH35 (Fig. 4C). Particularly strong MXRA5 signal was also noted in mesoderm immediately surrounding the nephric (mesonephric) duct although only little signal was observed within the mesonephros (Fig. 4D). In the HH35 limb bud MXRA5 exhibited restricted expression predominantly in developing wing joints. Transcripts in the forming elbow were detected in presumptive articular cartilages of the humeroulnar joint with less signal apparent in the early cavitation stage central lamina of the interzone (Fig. 4E). Interestingly, MXRA5 elbow localization displayed asymmetry with greater staining associated with the ventral trochlear aspect. Overall perichondrial MXRA5 transcripts in the limb increased with proximity to developing joints. Staining of perichondria associated with humeral and ulnar cartilages displayed differences in intensity particularly with respect to sides of the anlage. In the carpus, MXRA5 expression in the pre-cavitation stage joint was marked in the interzone and developing articular surfaces with similar signal intensity (Fig. 4F) and was particularly strong in the radiocarpal

joint (Fig. 4G). Toward the wrist, similar asymmetry also existed in perichondrial staining (Fig. 4F) as noted in the elbow.

HH38

In the HH38 heart MXRA5 was expressed strongly in remodeling atrioventricular and semilunar valve leaflets (Fig. 5 A-C). In AV valves (Fig. 5 A,B), there appeared asymmetric expression with cells of the septal leaflet expressing MXRA5 more strongly in the atrial layer along the AV canal whereas in other leaflets, more so within the proteoglycan rich interior of the valve (Combs and Yutzy, 2009). AV leaflets also showed transcript expression that extended into the adjacent myocardial wall. Cellular localization in semilunar valves in the cardiac outlet at this stage was also largely found within the interior portion of the valves (Fig. 5C). Elsewhere in the trunk, there was also strong MXRA5 signal intensity at several sites not noted at earlier stages to any great extent. Some of these areas included splanchnic mesoderm surrounding

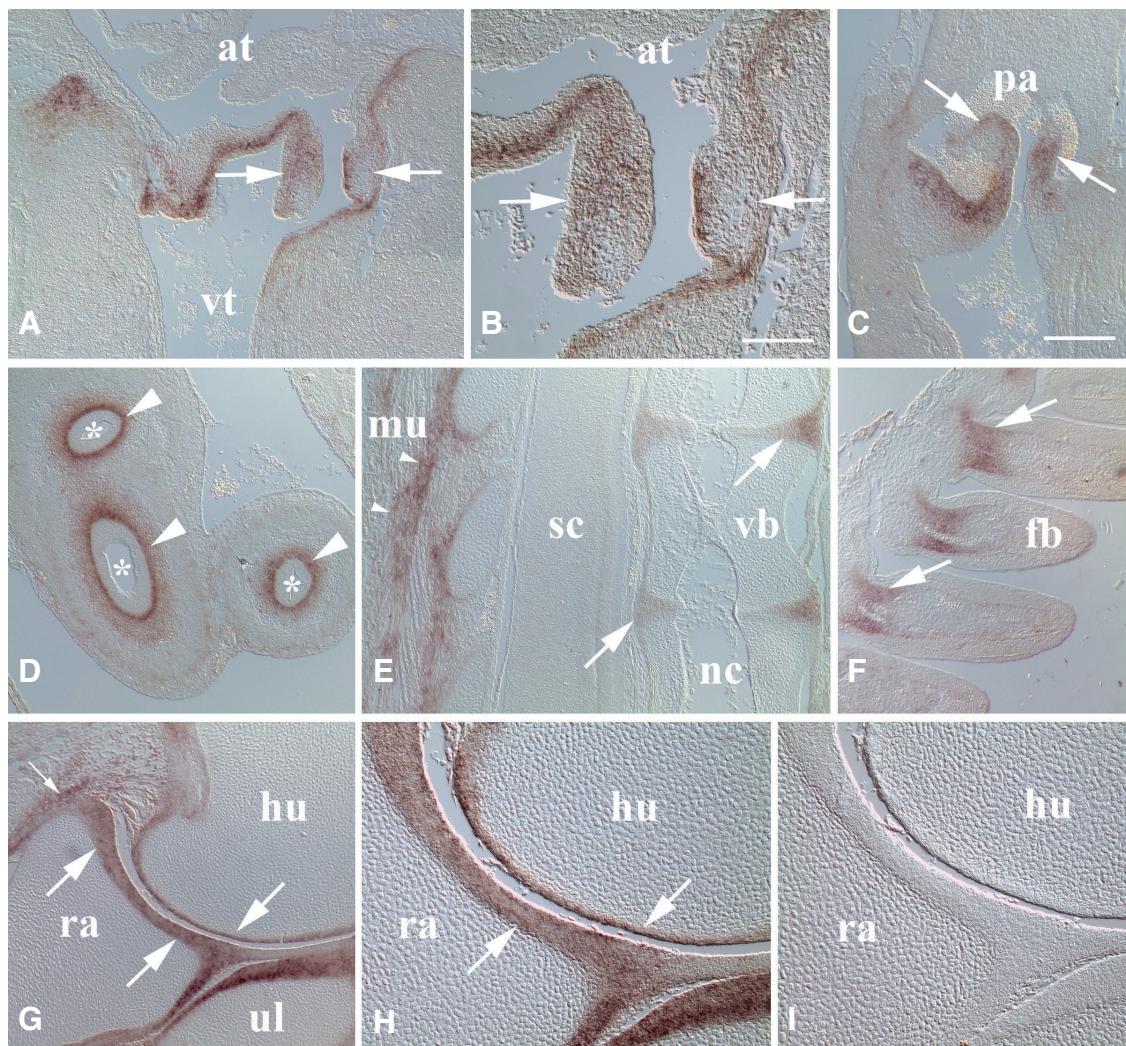


Fig. 5. MXRA5 transcript localization in the trunk and wing of the HH38 embryo. (A) In the heart, cells of the right atrioventricular valve leaflets displayed MXRA5 mRNA (arrows) extending into the underlying myocardium. at, atrium. vt, ventricle. (B) Higher magnification of atrioventricular valve shown in A. Note asymmetrical localization in valve leaflets with septal leaflet (right arrow) showing staining more restricted to superficial aspect. (C) Pulmonary semilunar valve leaflets also displayed transcript localization (arrows). pa, pulmonary artery. (D) Intestinal loops (asterisks) showed localization largely in splanchnic mesoderm forming lamina propria (large arrowheads) and extending into the submucosa. (E) MXRA5 mRNA was also found in the peripheral region of forming intervertebral discs (arrows) and in muscular (mu) attachments along the vertebral column (small arrowheads). Note lack of reactivity in spinal cord (sc), notochord (nc), and vertebral body cartilage (vb). (F) Expression (arrows) in the proximal dermal core of wing feather buds (fb). (G) MXRA5 was highly expressed in cells of humeroradial and humeroulnar articulations of the elbow joint (large arrows). Staining continued into the perichondrium and was strong at capsular ligament attachments (small arrow). hu, humerus. ra, radius. ul, ulna. (H) Higher magnification of elbow joint shown in G. Note sharply demarcated signal boundary (arrows) between maturing joint articular structure and underlying epiphyseal cartilages. (I) Control probe showed no reactivity with cells of the articular surfaces of the elbow joint. Scale bar in (B), 100 μ m for (B,H,I); bar in (C), 200 μ m for (A, C-G).

the intestine (Fig. 5D) which showed pronounced localization in the developing lamina propria and less signal in the underlying submucosa. Intervertebral discs (Fig. 5E) also showed MXRA5 mRNA expression, more so in cells of the outer annulus. As seen at earlier stages, sites of skeletal muscle attachment, in this case along the vertebral column, continued at HH38 as well. Interestingly, as in all stages examined earlier, no MXRA5 signal was detected in notochord, spinal cord or peripheral nerve fibers (Fig 5E). Feather buds also exhibited pronounced MXRA5 expression in cells of the dermal papillae surrounding central vasculature at the base of early feather follicles (Fig. 5F). In the wing at this stage, MXRA5 was most highly expressed in maturing joint structures particularly along the developing articular surfaces as seen in the elbow (Fig. 5 G,H). Articular cartilages of the humeroulnar, humeroradial and proximal radioulnar joints all showed robust localization and clearly delineated boundaries with the underlying epiphysis. Moreover, as noted at earlier stages, MXRA5 expression continued into the adjacent perichondrium. Sites of capsular ligamentous attachment showed increased MXRA5 transcript signal as well (Fig. 5G). As seen throughout the study control specimens incubated with sense probe during hybridization lacked reactivity in developing joint tissues (Fig. 5I).

Discussion

MXRA5 is an extracellular matrix protein whose pattern of expression has not been well characterized to date during embryonic development of avian trunk and limb. Transcript localization during early to mid-stages of chick development (HH18-38) revealed that it was largely expressed in cells of mesodermal origin. Furthermore, the extent of its expression appeared restricted to only a few sites during earlier stages and gradually expanded over the course of active organogenesis. Mesodermal derivatives that expressed MXRA5 were quite variable, ranging from specific subsets of gut-associated tissues including liver mesentery, esophageal adventitia, and connective tissues of the developing intestinal wall to cardiac valve rudiments, appendicular articulations, and dermal papillae of feather buds. In any event, a common theme was that onset of strongest MXRA5 expression in the trunk and limb correlated with remodeling of extracellular matrix (ECM) structure that occurs during transition from a provisional mesenchymal ECM into differentiated tissues.

Several areas of trunk and limb MXRA5 cellular expression also coincided with development of tendinous attachment points between skeletal muscle and vertebrae or aponeurotic attachments between individual segmental muscles. Moreover, developing tendon and ligamentous attachments to the perichondrium of the cartilage skeleton noted in limb suggested a possible role for MXRA5 in establishment of fibrocartilaginous tissues to provide needed strength and resilience required of these connections. Expression of MXRA5 in cells of the forming annulus fibrosus of the intervertebral disc offers support for the idea that its expression may facilitate development of this hybrid ECM. In developing chick diarthrodial joints MXRA5 expression co-distributed with that reported for versican proteoglycan (Shepard *et al.*, 2007) and strong MXRA5 localization in developing articular cartilages also correlated with establishment of a fibrocartilage-like matrix as previously described for avian synovial joint surfaces (Archer *et al.*, 1994). The question remains as to MXRA5's function in dif-

ferentiating connective tissues but putative interaction with latent transforming growth factor beta binding protein 2 (LTBP2; Bertoni *et al.*, 2016) suggests one potential role for MXRA5 in regulation of TGF β signaling pathways in establishment of different connective tissue matrices.

One of the most striking sites of MXRA5 expression was in forming valve tissues of the heart. Little staining for MXRA5 transcripts was noted elsewhere in the developing heart except in endocardial cushion mesenchyme and immediately associated heart wall at later stages. Interestingly, during early cushion epithelial - mesenchymal transformation stages little MXRA5 mRNA was noted, but at HH24/25 there was sudden appearance of transcripts in cushion mesenchyme immediately preceding onset of AV cushion tissue fusion at HH26 (Martinsen, 2005). During subsequent stages MXRA5 expression strengthened in developing valve leaflets as cushion mesenchyme underwent differentiation into the fibroblasts responsible for remodeling the valvular ECM. As with other sites of expression in the developing embryo it is tempting to speculate that MXRA5 may be involved with TGF β activation in maturing valve leaflets through interaction with LTBP2 (Bertoni *et al.*, 2016). Interestingly, LTBP2 is often associated with a fibrillin-enriched elastic ECM (Robertson *et al.*, 2015) which is also an important part of several developing connective tissues that also express MXRA5, including valve leaflets of the heart.

In summary, to our knowledge the present study has provided the first insight into MXRA5 gene expression in specific cell populations of the trunk and limb of early to mid-stage avian embryos. Results show that MXRA5 mRNA was expressed by cells at several sites during critically important developmental events involving transition of embryonic tissues into the adult morphology.

Materials and Methods

Chick embryos were fixed at stages HH18-38 in 85% ethanol, 10% formaldehyde, 5% glacial acetic acid, embedded in paraffin, and sectioned in sagittal plane at 10-11 μ m. Serial or closely neighboring sections were used for comparison between experimental and control samples. Results reported were from 2-6 separate experiments at each developmental stage. All experiments utilizing chick embryos were approved by the East Carolina University Institutional Animal Care and Use Committee.

In situ hybridization to localize MXRA5 transcripts in embryonic chick tissues was performed per Capehart and Kern (2003) and Cronin and Capehart (2007) with minor modification. Briefly, reverse transcriptase-polymerase chain reaction (RT-PCR) was performed to obtain MXRA5 transcripts from developing wings at HH35. RNA was isolated (RiboPure Kit, Applied Biosystems) and cDNA prepared (Superscript III, Invitrogen) per manufacturer's instructions. Forward and reverse primers used to amplify chick MXRA5 (XM_416583.3) cDNA were, respectively: 5'-AATTTACTC-CAGCAGCTTCATCC-3' and 5'-CATTGCCATGCTCATCAGTC-3' yielding a ~490-base pair amplicon. Amplicons were ligated into pGEMT-Easy (Promega) and sequenced for verification. Digoxigenin-labeled RNA antisense and sense probes were generated from NcoI and NdeI linearized plasmids using the MAXIscript *In vitro* Transcription Kit (Applied Biosystems) per manufacturer's instructions with substitution of kit NTPs by DIG RNA Labeling Mix (Roche). Labeled probes were quantified by dot blot and hybridization was performed overnight at 55°C in 2X SSC, 50% formamide, 10% dextran sulfate, 0.02% SDS, and 0.01% yeast tRNA containing 1 ng/ml antisense (experimental) or sense (control) probes. Sections were washed thoroughly in 1X SSC/50% formamide and equilibrated in Tris buffered saline (TBS). Specimens were incubated 1 hour room temperature in blocking buffer (Roche) containing 10% fetal calf and 1% sheep serum followed by 1:1000 sheep anti-digoxigenin-alkaline phosphatase (Roche) in blocking

buffer. After TBS washes, bound probe was visualized using nitroblue tetrazolium/5-bromo-4-chloro-3-indolyl-phosphate substrate (Roche).

Acknowledgements

The authors wish to thank the East Carolina University Department of Biology and National Institutes of Health Grant #HD040846. Thanks also to Matthew Whitford and Tyler Hartmann for assistance with histological preparation of tissue samples.

References

- ARCHER CW, MORRISON H, PITSILLIDES A (1994). Cellular aspects of the development of diarthrodial joints and articular cartilage. *J Anat* 184: 447-456.
- BALAKRISHNAN L, NIRUJOG RS, AHMAD S, BHATTACHARJEE M, MANDA SS, RENUSE S, KELKAR DS, SUBBANNAYYA Y, RAJU R, GOEL R, THOMAS JK, KAUR N, DHILLON M, TANKALA SG, JOIS R, VASDEV V, RAMACHANDRA YL, SAHASRABUDDHE NA, PRASAD TSK, MOHAN S, GOWDA H, SHANKAR S, PANDLEY A (2014). Proteomic analysis of human osteoarthritis synovial fluid. *Clin Proteomics* 11: 6-18.
- BERTONI N, PEREIRA LMS, SEVERINO FE, MOURA R, YOSHIDA WB, REIS PP (2016). Integrative meta-analysis identifies microRNA-regulated networks in infantile hemangioma. *BMC Med Genetics* 17: 4-14.
- BUCKANOVICH RJ, SASAROLI D, O'BRIEN JENKINS A, BOTBYL J, HAMMOND R, KATSAROS D, SANDALTOPOULOS, LIOTTA LA, GIMOTTY PA, COUKOS G (2007). Tumor vascular proteins as biomarkers in ovarian cancer. *J Clin Oncology* 25: 852-861.
- CAPEHART AA, KERN CB (2003). Identification of gamma A-like protocadherin expressed during chick development. *J Cell Biochem* 90: 608-618.
- COMBS MD, YUTZEY KE (2009). Heart valve development: Regulatory networks in development and disease. *Circ Res* 105: 408-421.
- CRONIN KD, CAPEHART AA (2007). Gamma protocadherin expression in the embryonic chick nervous system. *Int J Biol Sci* 3: 8-11.
- DOLAN J, WALSHE K, ALSBURY S, HOKAMP K, O'KEEFE S, OKAFUJI T, MILLER SFC, TEAR G, MITCHELL KJ (2007). The extracellular leucine-rich repeat superfamily; a comparative survey and analysis of evolutionary relationships and expression patterns. *BMC Genomics* 8: 320-344.
- HAMBURGER V, HAMILTON HL (1951). A series of normal stages in the development of the chick embryo. *J Morphol* 88: 49-92.
- HE Y, CHEN X, LIU H, XIAO H, KWAPONG WR, MEI J (2015). Matrix-remodeling associated 5 as a novel tissue biomarker predicts poor prognosis in non-small cell lung cancers. *Cancer Biomark* 15: 645-651.
- JOYCE NC, HARRIS DL, MARKOV V, ZHANG Z, SAITTAB (2012). Potential of human umbilical cord mesenchymal stem cells to heal damaged corneal endothelium. *Mol Vision* 18: 547-564.
- KONG B-W, LEE JY, BOTTJE WG, LASSITER K, LEE J, FOSTER DN (2011) Genome-wide differential gene expression in immortalized DF-1 chicken embryo fibroblast cell line. *BMC Genomics* 12: 571-590.
- MARTINSEN BJ (2005). Reference guide to the stages of chick heart embryology. *Dev Dynamics* 233: 1217-1237.
- NAGCHOWDHURI PS, ANDREWS KN, ROBARTS, CAPEHART AA (2012). Versican knockdown reduces interzone area during early stages of chick synovial joint development. *Anat Rec* 295: 397-409.
- ROBERTSON IB, HORIGUCHI M, ZILBERBERG L, DABOVIC B, HADJIOLOVA K, RIFKIN DB (2015). Latent TGF- β -binding proteins. *Matrix Biol* 47: 44-53.
- SHEPARD JB, KRUG HA, LAFOON BA, HOFFMAN S, CAPEHART AA (2007). Versican expression during synovial joint morphogenesis. *Int J Biol Sci* 3: 380-384.
- SOULET F, KILARSKI WW, ROUX-DALVAI F, HERBERT JMJ, SACEWICZ I, MOUTON-BARBOSA E, BICKNELL R, LALOR P, MONSARRAT B, BIKFALVI A (2013). Mapping the extracellular and membrane proteome associated with the vasculature and the stroma in the embryo. *Mol Cell Proteomics* 12: 2293-2312.
- WALKER MG, VOLKMUTH W (2002). Cell adhesion and matrix remodeling genes identified by co-expression analysis. *Gene Funct Dis* 3: 109-112.
- YU M, YUE Z, WU P, WU DY, MAYER JA, MEDINA M, WIDELITZ RB, JIANG TX, CHUONG CM (2004). The developmental biology of feather follicles. *Int J Dev Biol* 48: 181-191.
- ZOU TT, SELARU FM, XU Y, SHUSTOVA V, YIN J, MORI Y, SHIBATA D, SATO F, WANG S, OLARU A, DEACU E, LIU TC, ABRAHAM JM, MELTZER SJ (2002). Application of cDNA microarrays to generate a molecular taxonomy capable of distinguishing between colon cancer and normal colon. *Oncogene* 21: 4855-4862.

Further Related Reading, published previously in the *Int. J. Dev. Biol.*

SDF-1 controls the muscle and blood vessel formation of the somite

Aisha Abduelmula Ruijin HuangQin Pu, Hirokazu Tamamura, Gabriela Morosan-Puopolo and Beate Brand-Saberi
Int. J. Dev. Biol. (2016) 60: 29-38
<https://doi.org/10.1387/ijdb.150132rh>

Cytoskeletal heart-enriched actin-associated protein (CHAP) is expressed in striated and smooth muscle cells in chick and mouse during embryonic and adult stages

Willemijn van Eldik, Abdelaziz Beqqali, Jantine Monshouwer-Kloots, Christine Mummy and Robert Passier
Int. J. Dev. Biol. (2011) 55: 649-655
<https://doi.org/10.1387/ijdb.103207wv>

Generation of pattern and form in the developing limb

Matthew Towers and Cheryll Tickle
Int. J. Dev. Biol. (2009) 53: 805-812
<https://doi.org/10.1387/ijdb.072499mt>

A comparative analysis of Meox1 and Meox2 in the developing somites and limbs of the chick embryo

Susan Reijntjes, Sigmar Stricker and Baljinder S. Mankoo
Int. J. Dev. Biol. (2007) 51: 753-759
<https://doi.org/10.1387/ijdb.072332sr>

The expression of Flrt3 during chick limb development

Terence G. Smith and Cheryll Tickle
Int. J. Dev. Biol. (2006) 50: 701-704
<https://doi.org/10.1387/ijdb.062192ts>

Programmed cell death in the developing limb

Vanessa Zuzarte-Luís and Juan M Hurlé
Int. J. Dev. Biol. (2002) 46: 871-876
<http://www.intjdevbiol.com/web/paper/12455623>

Developmental expression of chick twist and its regulation during limb patterning

A T Tavares, J C Izpisúja-Belmonte and J Rodriguez-León
Int. J. Dev. Biol. (2001) 45: 707-713
<http://www.intjdevbiol.com/web/paper/11669372>

5 yr ISI Impact Factor (2016) = 2.421

